0026-895X/07/7205-1258–1268$20.00
MOLECULAR PHARMACOLOGY
Copyright © 2007 The American Society for Pharmacology and Experimental Therapeutics
*Mol Pharmacol* 72:1258–1268, 2007

Vol. 72, No. 5
37044/3263402
*Printed in U.S.A.*



# Pharmacological Characterization and Molecular Determinants of the Activation of Transient Receptor Potential V2 Channel Orthologs by 2-Aminoethoxydiphenyl Borate[S]

Véronique Juvin, Aubin Penna, Jean Chemin, Yea-Lih Lin, and François-A. Rassendren

*Department of Molecular Pharmacology, Institut de Génomique Fonctionnelle, Montpellier, France (V.J., A.P., F-A.R.); Department of Physiology, Institut de Génomique Fonctionnelle, Montpellier, France (J.C.); Centre National de la Recherche Scientifique, Unité Mixte de Recherche 5203, Montpellier, France (V.J., A.P., J.C., F-A.R.); Institut National de la Santé et de la Recherche Médicale, U661, Montpellier, France (V.J., A.P., J.C., F.-A.R.); Université de Montpellier (IFR3), Montpellier, France (V.J., A.P., J.C., F.-A.R.); Institut de Génétique Humaine, Montpellier, France (Y.-L.L.); Centre National de la Recherche Scientifique UPR1142, Montpellier, France (Y.-L.L.)*

Received April 12, 2007; accepted August 2, 2007

## ABSTRACT

Despite its expression in different cell types, transient receptor potential V2 (TRPV2) is still the most cryptic members of the TRPV channel family. 2-Aminoethoxydiphenyl borate (2APB) has been shown to be a common activator of TRPV1, TRPV2, and TRPV3, but 2APB-triggered TRPV2 activation remains to be thoroughly characterized. In this study, we have developed an assay based on cell lines stably expressing mouse TRPV2 channels and intracellular calcium measurements to perform a pharmacological profiling of the channel. Phenyl borate derivatives were found to activate mouse TRPV2 with similar potencies and thus were used to screen a panel of channel blockers. Besides the classic TRP inhibitors ruthenium red (RR) and 1-(β-[3-(4-methoxyphenyl) propoxy]-4-methoxyphenethyl)-1*H*-imidazole hydrochloride (SKF96365), two potassium channel blockers, tetraethylammonium (TEA) and 4-aminopyridine, and an inhibitor of capacitative calcium entry, 1-(2-(trifluoromethyl) phenyl) imidazole (TRIM), were found to inhibit TRPV2 activation by 100 μM 2APB. Activation by 300 μM 2APB, however, could only be inhibited by RR and TRIM. Electrophysiological recordings demonstrated that TEA inhibition was use-dependent, suggesting that high concentrations of 2APB might induce a progressive conformational change of the channel. Comparison of TRPV2 orthologs revealed that the human channel was insensitive to 2APB. Analysis of chimeric constructs of mouse and human TRPV2 channels showed that the molecular determinants of 2APB sensitivity could be localized to the intracellular amino and carboxyl domains. Finally, using lentiviral-driven expression, we demonstrate that hTRPV2 exerts a dominant-negative effect on 2APB activation of native rodent TRPV2 channels and thus may provide an interesting tool to investigate cellular functions of TRPV2 channels.

Transient receptor potential (TRP) proteins are cationic channels that were first discovered in *Drosophila melanogaster*, in which they play a crucial role in the initial steps of visual transduction (Hardie, 2001; Montell, 2005a). Since then, more than 30 mammalian TRP channels have been identified and are classified into seven families, which are TRPC, TRPV, TRPM, TRPN, TRPA and the two distantly related TRPP and TRPML (Montell, 2005b). All members of the TRP superfamily share the same membrane topology as voltage-gated potassium channels; they contain six hydrophobic domains spanning the plasma membrane and an additional P-loop structure between the fifth and the sixth transmembrane segments that participates in the pore-forming domain of the channel. TRP proteins possess long cyto-

This work was supported in part by Centre National de la Recherche Scientifique and Institut National de la Santé et de la Recherche Médicale. J.V. and P.A. were supported by student fellowships from Association de la Recherche sur le Cancer.

Article, publication date, and citation information can be found at http://molpharm.aspetjournals.org.

doi:10.1124/mol.107.037044.

[S] The online version of this article (available at http://molpharm.aspetjournals.org) contains supplemental material.

**ABBREVIATIONS:** TRP, transient receptor potential; 2APB, 2-aminoethoxydiphenyl borate; DPBA, diphenylboronic anhydride; RBL-2H3, rat basophilic leukemia clone 2H3; RR, ruthenium red; TEA, tetraethlyammonium; 4-AP, 4-aminopyridine; TRIM, 1-(2-(trifluoromethyl)phenyl) imidazole; TMD, transmembrane domain; THC, $\Delta^9$-tetrahydrocannabinol; SKF96365, 1-(β-[3-(4-methoxyphenyl) propoxy]-4-methoxyphenethyl)-1*H*-imidazole hydrochloride; HA, hemagglutinin; GFP, green fluorescent protein; CHO, Chinese hamster ovary; HEK, human embryonic kidney; PBS, phosphate-buffered saline; AM, acetoxymethyl ester; HBSS, Hanks' balanced salt solution; BSA, bovine serum albumin; BK8644, 1,4-dihydro-2,6-dimethyl-5-nitro-4-(2-(trifluoromethyl)phenyl)-3-pyridinecarboxylic acid, methyl ester; SKF96365, 1-(β-[3-(4-methoxyphenyl)propoxy]-4-methoxyphenethyl)-1*H*-imidazole.

plasmic amino and carboxyl termini, in which structural motifs such as ankyrin repeats or coiled-coil domains are often conserved. Although the structure of TRP channels is still unresolved, they seem to assemble as tetramers, as do potassium channels (Ramsey et al., 2006).

All TRP channels are permeable to cations, but ionic selectivities and modes of gating are extremely diverse; to add to this complexity, a given TRP can be activated by different stimuli, depending on either the cell type in which it is expressed or the subcellular-specific signaling complex associated with the channel (Clapham, 2003). Hence, studying TRP channel gating is still very challenging and prone to controversy. One unifying view is that these channels are tightly regulated by various cellular second messengers, such as lipids, kinases, and calcium, but also by dynamic protein-protein interactions; these regulations may underlie the ability of TRP channels to endorse a variety of cellular functions.

As yet, the precise cellular functions of most TRP channels remain unresolved, because the lack of specific pharmacological tools combined with their complex mode of gating represent a considerable obstacle to physiological studies. However, it is now clear that a subset of TRP channels is involved in sensory transduction (Clapham, 2003). Indeed, different sensory stimuli, in particular heat or cold, activate TRPVs 1 to 4, TRPM8, or TRPA proteins (Tominaga and Caterina, 2004). Several endogenous substances and pharmacologically active molecules are TRPV channel agonists. In particular TRPV1, -3, and -4 are gated by bioactive lipids such as phosphatidylinositol bisphosphate or fatty-acid derivatives (Benham et al., 2002). Although TRPV1, -3, and -4 channels act unambiguously as cellular temperature sensors and are gated or modulated by lipids, the gating of TRPV2 (initially named VRL-1) is still a matter of debate. Indeed, the temperature threshold for TRPV2 activation (>50°C) (Caterina et al., 1999) is well above physiological range, and this channel has not been demonstrated to be sensitive to lipids. In addition, in non-neuronal cells, other mechanisms have been reported to activate TRPV2, such as dynamic insertion in the plasma membrane (Kanzaki et al., 1999), regulation by a PI3-kinase dependent pathway (Penna et al., 2006) or mechano- and osmotic stimuli (Iwata et al., 2003; Muraki et al., 2003). 2APB and its derivative diphenylboronic anhydride (DPBA) have been shown to be potent activators of TRPV1, TRPV2, and TRPV3 (Hu et al., 2004). Although activation of TRPV1 and TRPV3 channels by 2APB has been characterized in some detail (Chung et al., 2004), there are few data available on its effect on TRPV2 channels. In this study, we provide a characterization of the activation of TRPV2 channel orthologs (mouse, rat, human) by 2APB. We show that 2APB activates mouse and rat TRPV2 orthologs with different potencies, whereas the human TRPV2 channel is remarkably insensitive to 2APB. Through chimeric constructs of mouse and human TRPV2 channels, we have identified the molecular determinants of 2APB sensitivity. We also investigated the potential cellular function of endogenous TRPV2 expressed in RBL-2H3 cells using a lentiviral-mediated expression of a dominant-negative human TRPV2 channel.

## Materials and Methods

**Reagents and Antibodies.** All chemicals were purchased from Sigma-Aldrich (St. Louis, MO), except for 2APB, which was from Calbiochem (San Diego, CA). Culture media and reagents were obtained from Invitrogen (Carlsbad, CA); endotoxin free-fetal calf serum used for RBL-2H3 was from Biowest (Miami, FL).

**Epitope Tagging, Mutagenesis, and Construction of Chimeras.** Insertions of Flag and HA tags in hTRPV2 and site-directed mutagenesis have been described previously (Penna et al., 2006). Mutations introduced in the selectivity filter of hTRPV2 were E599K, M607K, and E609K. Because of the high sequence homology between human and mouse TRPV2 cDNAs, chimeras were constructed by introducing unique silent restriction sites by oligonucleotide-directed mutagenesis in both cDNAs. Sites inserted were the following: SacII between Lys390 and Phe391, Bsu36I between Arg537 and Phe538, EcoRI between Val649 and Asn650, BspeI between Ser726 and Gly727 for human TRPV2; SacII between Arg387 and Phe388, Bsu36I between Arg534 and Phe535, EcoRI between Val644 and Asn645, and BspeI between Ser722 and Gly723 for mouse TRPV2. After restriction digestion, human and mouse fragments were swapped. All of the clones were verified by sequencing.

**Lentiviral Vector Construction and Production.** cDNAs coding for human flag-TRPV2$^{HA}$ and mutant human flag-TRPV2$^{HA}$ channels were cloned in front of an IRES-GFP cassette into the lentiviral expression vector pWPXL (Klages et al., 2000). To produce GFP- and hTRPV2-harboring human immunodeficiency virus vectors, pWPXL-GFP or pWPXL-hTRPV2 plasmids were cotransfected in HEK 293T cells with the human immunodeficiency virus packaging plasmid p8.2 and the plasmid pMD.G that encodes the vesicular stomatitis virus glycoprotein envelope. Viruses were harvested and concentrated, and titers were calculated as described previously (Naldini et al., 1996).

**Cell Culture, Transfection, and Viral Transduction.** Chinese hamster ovary cells (CHO-K1, American Type Culture Collection number CCL-61) and rat basophilic leukemia cells (RBL-2H3; gift from Dr U. Blank, Institut Pasteur, Paris, France) were grown in Ham's F-12 medium and Dulbecco's modified Eagle's medium, respectively, supplemented with 10% fetal calf serum, 1% GlutaMAX, 100 IU/ml penicillin, and 100 $\mu$g/ml streptomycin at 37°C in a humidified 5% $CO_2$ incubator. For stable CHO cell lines expressing mouse TRPV2 (clone IIE11), 200 $\mu$g/ml G418 was added to the culture medium but omitted for experiments. HEK-293 cells (American Type Culture Collection number CCL-1573) were grown in Dulbecco's modified Eagle's medium supplemented with 10% fetal calf serum, 1% GlutaMAX, 100 IU/ml penicillin, and 100 $\mu$g/ml streptomycin.

CHO and HEK-293 cells were transfected using AMAXA system (AMAXA Inc., Gaithersburg, MD) or jetPEI (PolyPlus Transfection Inc., New York, NY), respectively, according to the manufacturers' instructions. Cells were used 48 h after transfection.

For viral transduction, CHO, clone IIE11, or RBL-2H3 cells were plated at $2.5 \times 10^5$ cells/well (12-well plates). Lentiviral vectors were then added to the cell cultures at a multiplicity of infection of 40, along with 8 $\mu$g/ml Polybrene (Sigma). Cell cultures were then centrifuged at 300*g* for 60 min at 30°C, incubated for 18 h at 37°C in a humidified 5% $CO_2$ incubator, and then washed twice in PBS. Experiments were performed at least 5 days after transduction. In a typical experiment, 95% of the cells were transduced.

**Intracellular Calcium Measurements.** For Fluo-4/AM calcium measurements, CHO or RBL-2H3 cells were plated on poly(ornithine)-coated 96-well plates at a density of $5 \times 10^4$ cells/well. Plates were washed three times in Hanks' balanced salt solution (HBSS) containing 142 mM NaCl, 5.6 mM KCl, 1 mM $MgCl_2$, 2 mM $CaCl_2$, 0.34 mM $Na_2HPO_4$, 0.44 mM $KH_2PO_4$, 10 mM HEPES, and 5.6 mM glucose, 310 mOsM, pH 7.4. Cells were then incubated in HBSS supplemented with 2.5 mM probenecid (Sigma), 100 $\mu$g/ml pluronic acid and 1 $\mu$M Fluo-4/AM (both from Invitrogen) for 1 h at 37°C. After the incubation, cells were washed twice with HBSS. Intracellular calcium measurements were performed on a fluorescence plate reader (FlexStation II; Molecular Devices, Sunnyvale, CA), and drugs were applied at 2× using a fluid-handling integrated device.

All measurements were performed in triplicate at 30°C. For analysis, the fluorescence signal was integrated over a 1-min period.

**Immunocytochemistry.** TRPV2 immunostaining was performed 48 h after transfection. Cells were fixed in 4% paraformaldehyde for 10 min, washed in 0.1 M glycine, blocked in PBS with 0.5% BSA for 30 min, permeabilized using 0.05% Triton X-100 for 5 min, and incubated with primary antibody in blocking solution overnight at 4°C. After PBS with 0.5% BSA washes, cells were incubated with fluorescent secondary antibody for 30 min at 37°C. Fluorescence was visualized on a Leica DMRA2 epifluorescent microscope using a 63× oil-immersion objective (Leica Microsystems, Inc., Deerfield, IL). Images were acquired using a cool-snap HQ (photometric) digital camera. Image deconvolution was performed as described previously (Penna et al., 2006). mTRPV2 was detected using anti-VRL-1 antibody (1/50) (EMD Biosciences, San Diego, CA), hTRPV2 was detected using a specific rabbit antibody (1/250) produced in the laboratory and Flag-tagged with anti-Flag (M2) monoclonal antibody (1/1000) from Sigma. Because of sequence divergences between mouse and human TRPV2, we checked that each antibody was species-specific (data not shown). Secondary antibodies were Alexa Fluor 488 anti-rabbit antibody (1/2000) from Invitrogen, and Cy3-conjugated anti-mouse antibody (1/1000) was from Jackson ImmunoResearch Laboratories Inc. (West Grove, PA).

**Western Blotting.** Cells were lysed in 200 μl of lysis buffer [20 mM HEPES, 100 mM NaCl, 5 mM EDTA, 1% Triton X-100, and protease inhibitor cocktail (Roche, Indianapolis, IN), pH 7.4] and passed five times through a 26-gauge needle. After 30 min of solubilization at 4°C under agitation, lysates were centrifuged (16,000*g*, 10 min, 4°C). Protein extracts were diluted in 6× Laemmli buffer, resolved by SDS-polyacrylamide gel electrophoresis, and transferred to nitrocellulose membranes. Blocking was performed using 5% nonfat dry milk in Tris-buffered saline containing 0.05% Tween 20 followed by incubation with the primary antibody in the blocking buffer at 4°C overnight. Antibody dilutions were anti-VRL-1, 1/250; anti-hTRPV2, 1/500; anti-GFP, 1/2500 (Torrey Pines Biolabs, Houston, TX); horseradish peroxidase-conjugated anti-Flag (M2) antibody, 1/4000 (Sigma); and anti-tubulin, 1/2000 (Sigma). After a 30-min wash with Tris-buffered saline containing 0.05% Tween 20, membranes were incubated for 1 h in either anti-rabbit (1/10,000) or anti-mouse (1/25,000) horseradish peroxidase-conjugated secondary antibodies from GE Healthcare (Chalfont St. Giles, Buckinghamshire, UK) and Pierce (Rockford, IL), respectively. Proteins were detected using a chemoluminescence detection kit (Pierce).

**Electrophysiological Recordings.** HEK-293 cells were plated at a density of $2 \times 10^5$ cells in individual 35-mm culture dishes. Macroscopic currents were recorded at room temperature (~22°C) by the whole-cell patch-clamp technique using an Axopatch 200B amplifier (Molecular Devices). The extracellular solution contained 150 mM NaCl, 5 mM KCl, 2 mM $CaCl_2$, 1 mM $MgCl_2$, and 10 mM HEPES, with pH adjusted to 7.35 with NaOH (330 mOsM). Borosilicate glass pipettes had a resistance of 1.5 to 2.5 MΩ when filled with an internal solution containing 140 mM CsCl, 10 mM EGTA, 10 mM HEPES, 3 mM magnesium-ATP, 0.6 mM GTP-sodium, and 2 mM $CaCl_2$, with pH adjusted to 7.2 with KOH (~315 mOsM). Drugs were applied by a perfusion system controlled by solenoid valves allowing a complete exchange of solution in less than 1 s. Recordings were filtered at 2 kHz. Data were analyzed using pClamp 9 (Molecular Devices) and Prism (GraphPad Software Inc., San Diego, CA) software. One-way analysis of variance combined with a Newman-Keuls post test were used to compare the different values and were considered significant at $p < 0.05$. Results are presented as mean current amplitudes (in picoamperes) or current densities (picoamperes per picofarad) (i.e., amplitudes normalized relative to cell membrane capacitance determined for each cell) ± S.E.M., and $n$ is the number of cells used.

***β*-Hexosaminidase Release Assays.** β-Hexosaminidase is a granule-associated enzyme that degrades glucosamine residues stored in secretion granules in mast cells. It is released in the extracellular medium when degranulation is triggered by physiological or chemical stimuli. Hence, a colorimetric assay of extracellular β-hexosaminidase can provide an indirect measurement of mast cell degranulation. RBL-2H3 cells were plated in 96-well plates at $5 \times 10^4$ cells/well and sensitized overnight at 37°C with anti-DNP IgE antibody (1/1000) from Sigma. Cells were washed three times in PBS and incubated for 30 min at 37°C in 50 μl of Locke buffer (140 mM NaCl, 1.2 mM $KH_2PO_4$, 5 mM KCl, 1.2 mM $MgSO_4$, 10 mM glucose, 10 mM HEPES, 1.8 mM $CaCl_2$, and 0.5% BSA; pH was adjusted to 7.4 using NaOH) containing either DNP-HSA or 2APB. PMA (50 nM) or ionomycin (200 nM) was used as a positive control to induce secretion. After stimulation, 20 μl of supernatant was incubated for 90 min at 37°C in 50 μl of citrate buffer (49.5% of 0.05 M citrate acid and 50.5% of 0.05 M trisodium citrate, pH 4.5) containing 1.3 mM *p*-nitrophenyl-*N*-acetyl-β-D-glucosamine. The reaction was stopped by adding 150 μl of glycine (0.2 M, pH 10.7). Total cellular content of β-hexosaminidase was determined after cell lysis in 0.5% Triton X-100 and directly assayed in the 96-well plates. Absorbance was determined at 410 nm in a microtiter plate reader. Results were expressed as a percentage of total β-hexosaminidase cellular content after correction for spontaneous release in unstimulated cultures. Each measurement was made in triplicate.

**Data Analysis.** The dose-response curves for agonist and inhibitors were fitted using GraphPad Prism. All data are mean ± S.E.M. from at least three individual experiments performed in triplicate. For dose-response curve experiments, $EC_{50}$ or $IC_{50}$ values were calculated for each individual experiment using the sigmoid dose-response equation with variable slope from PRISM, and values were averaged.

## Results

**2APB and DPBA Induce Calcium Influx through Mouse TRPV2 Channels.** We reported previously that transient transfection of TRPV2 cDNA can result in high levels of protein expression, leading to cellular toxicity (Penna et al., 2006). To avoid this problem, we generated monoclonal stable CHO cell lines expressing mouse TRPV2 channels (mTRPV2). Two clones (IB11 and IIE11) were selected based on moderate expression levels of TRPV2 and correct localization of the protein at the plasma membrane (Fig. 1). Because of the lower expression of TRPV2 in clone IIE11 compared with clone IB11, clone IIE11 was selected for all experiments in this study, unless indicated.

Phenyl-borate derivatives 2APB and DPBA have been shown to activate TRPV1, TRPV2, and TRPV3 (Hu et al., 2004). Here we used a fluorimetric calcium assay to perform a more precise pharmacological characterization of the activation of mTRPV2 by 2APB and DPBA. Both molecules induced a dose-dependent calcium increase in mTRPV2 stable cell line. The threshold for activation was 30 and 10 μM for 2APB and DPBA, respectively (Fig. 1B), and significant calcium signals were obtained at 100 μM; saturation was reached at doses greater than 1 mM. A high background signal was observed in parental cells for agonist concentrations greater than 300 μM. In these conditions, $EC_{50}$ values were 160 ± 26 ($n = 4$) and 105 ± 10 μM ($n = 4$) for 2APB and DPBA, respectively. Because at 100 and 300 μM, 2APB and DPBA induced little if any calcium signals in nontransfected cells, these two concentrations were used in all further experiments, unless indicated.

**Screening for mTRPV2 Channel Blockers.** We used our assay to screen a panel of small molecules that are known to inhibit ion channels, including known TRP channel blockers, small inorganic cations, other cationic channel blockers,

and calcium channel antagonists (see Supplementary Fig. S1). In a first step, a single concentration of these molecules was tested on calcium signals induced by 100 $\mu$M 2APB. As expected, the nonspecific TRP blockers ruthenium red (RR) and SKF96365 (both 100 $\mu$M) inhibited 2APB-mediated calcium signals in TRPV2-expressing cells. Inhibition levels were 96 ± 3% ($n$ = 3) and 78 ± 7% ($n$ = 3) for RR and SKF96365, respectively. The small inorganic trivalent cations $La^{3+}$ and $Gd^{3+}$ (both 100 $\mu$M), which block some TRP channels, were unable to block 100 $\mu$M 2APB-induced calcium signals. Similar results were obtained with 100 $\mu$M $Ni^{2+}$, $Cd^{2+}$, $Zn^{2+}$, hexamethonium, and the dihydropyridines nifedipine or BK8644 (racemic mixture) (Fig. 2A). On the contrary, the potassium channel blockers 4-aminopyridine (4-AP) (5 mM) and tetraethylammonium (TEA) (10 mM) induced inhibitions of 70 ± 6% ($n$ = 4) and 74 ± 6% ($n$ = 3), respectively. Finally, we found that 500 $\mu$M 1-(2-trifluoromethylphenyl) imidazole (TRIM), an inhibitor of nitric-oxide synthase and of capacitative calcium entry (Gibson et al., 2001; Tobin et al., 2006) reduced 100 $\mu$M 2APB-evoked responses by 62 ± 9% ($n$ = 3).

Complete inhibitory dose-response curves for RR, SKF96365, TEA, 4-AP, and TRIM were determined on 100 $\mu$M 2APB-induced responses (Fig. 2B, ▲). $IC_{50}$ values were RR, 7 ± 2 $\mu$M ($n$ = 4); SKF96365, 21 ± 16 $\mu$M ($n$ = 4); 4-AP, 2 ± 0.2 mM ($n$ = 3); and TEA, 1 ± 1 mM ($n$ = 3). However, when similar inhibitory dose responses were performed using 300 $\mu$M 2APB to activate TRPV2, a total loss of inhibition was observed for most of the molecules tested. Only RR was still effective ($IC_{50}$ = 12 ± 1 $\mu$M, $n$ = 4) (Fig. 2B, ■), as well as TRIM, albeit with an apparently lower potency.

Because several of the molecules that inhibit activation of TRPV2 by 2APB are traditionally known to be voltage-dependent open-channel blockers of their primary targets, we questioned whether their lack of effect on 300 $\mu$M 2APB-evoked responses could be related to such biophysical properties. Indeed, high 2APB concentrations could depolarize the membrane, thus reducing block of TRPV2 by open-channel blockers. On the other hand, 2APB could induce use-dependent conformational changes that may reduce the accessibility of the antagonists to their binding site. Using whole-cell recordings, we therefore analyzed whether the inhibition of 2APB-induced currents by 3 mM TEA showed any voltage-dependence and/or use-dependence. Because TRPV2 currents are of small magnitude when evoked by 2APB concentrations lower than 1 mM (Hu et al., 2004), these experiments were performed using HEK cells transiently transfected with mTRPV2 to provide a robust expression of TRPV2, and 3 mM 2APB was used to activate the channel to maximize current densities. Under these conditions, 3 mM 2APB evoked robust currents only in transfected cells, which displayed an activation time constant of 3.1 ± 0.3 s ($n$ = 20) and an inactivation time constant of 4.3 ± 0.4 s ($n$ = 20) (Fig. 3A). 2APB-induced currents did not show marked desensitization during agonist application or after repeated stimulation (Fig. 3A). TEA blocking efficacy was evaluated using two stimulation paradigms; in the first, 2APB was first applied alone and then coapplied with TEA. In this situation, although TEA significantly decreased 2APB currents, an important component of current remained unaffected by TEA (Fig. 3, B and D), and sometimes no inhibition at all could be obtained (Fig. 3B). In the second stimulation paradigm, TEA and 2APB were first coapplied, and then 2APB was applied alone. When cells were exposed to this sequence of application, 2APB-evoked currents were almost completely inhibited by TEA; current densities measured at −50 mV were not significantly different from those of control (Fig. 3, C and E). TEA inhibition of 2APB-evoked currents occurred similarly over the entire voltage range tested, indicating a lack of voltage dependence (Fig. 3C). Taken together, these results show that TEA block is use-dependent but not voltage-dependent, suggesting that 2APB

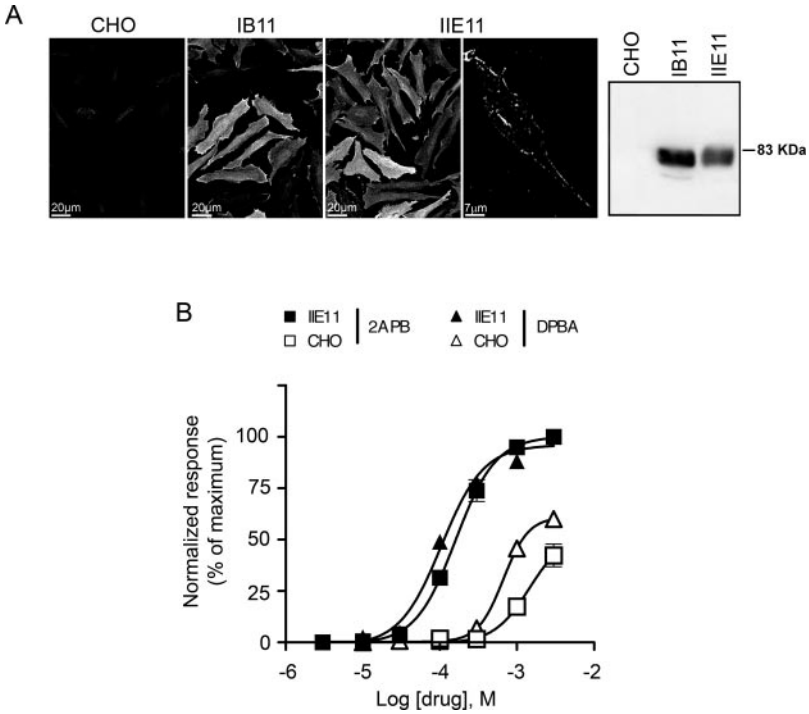


**Fig. 1.** 2APB and DPBA activate mouse TRPV2 stably expressed in CHO cells. A, immunostaining (left) and Western blot (right) showing expression of mTRPV2 in two monoclonal CHO cell populations. Immunostaining and image deconvolution (fourth on the right) clearly show the membrane localization of mTRPV2 in clones IB11 and IIE11. Western blot analysis confirmed the lack of expression of TRPV2 in parental CHO cells. B, dose-response curve for 2APB- and DPBA-induced calcium signals in clone IIE11 and parental CHO cells. Intracellular calcium measurements were performed using the calcium-sensitive probe Fluo-4/AM on a Flexstation II (Molecular Devices). For comparison purposes, fluorescence signals were normalized to the maximal response induced by 3 mM 2APB, and independent experiments were averaged. Note that both agonists induced intracellular calcium signals in parental cells at concentrations greater than 1 mM.

is likely to induce progressive conformational changes of the channel that are responsible for the reduced block in the presence of higher concentrations of 2APB.

**TRPV2 Orthologs Display Different 2APB Sensitivities.** The effects of 2APB were also investigated on calcium responses mediated by rat and human TRPV2 channel orthologs. For comparison purposes, the three cDNAs were cloned in the same expression vector and were transiently transfected in CHO cells. As shown in Fig. 4A, rat, mouse, and human TRPV2 channels display significant differences in their apparent affinity for 2APB. Rat TRPV2 was the most sensitive with an $EC_{50}$ value of 59 ± 13 μM ($n$ = 4) followed by mTRPV2, with an $EC_{50}$ of 187 ± 20 μM ($n$ = 4) (Fig. 4A). We were surprised to find that activation of the human channel with 2APB could not be obtained, despite its correct expression in the plasma membrane (Fig. 5). Similar differences in DPBA sensitivity were observed between TRPV2 orthologs and in transiently transfected HEK cells (data not shown).

We next sought to determine whether the 2APB insensitivity of hTRPV2 could affect 2APB activation of the mouse channel when both subunits are associated within the channel complex. Different ratios of cDNA coding for both channels were cotransfected; the amount of mTRPV2 cDNA was kept constant, whereas that of hTRPV2 was increased. Calcium signals induced by 100 and 300 μM 2APB were measured in each condition. As shown in Fig. 4B, increasing the amount of hTRPV2 cDNA dose-dependently reduced the 2APB-mediated calcium signal. At 100 μM 2APB, a 67 ± 2% ($n$ = 4) reduction of the response was observed when the ratio of m/h TRPV2 was 1:3, and maximal inhibition (90 ± 2%, $n$ = 4) was achieved for a ratio of 1:7. At 300 μM 2APB, levels of inhibition were lower (ratio 1:3, 37 ± 4%, $n$ = 4; ratio 1:7, 65 ± 2%, $n$ = 4; ratio 1:10, 72 ± 1%, $n$ = 4) but significantly different from control ($p < 0.0001$, unpaired Student's $t$ test). These results show that both human and mouse TRPV2 subunits can form heteromeric channels and that the presence of a human subunit impairs the activation of the composite channel by 2APB. Complete inhibition could not be reached, presumably because of the presence of homomeric mTRPV2 channels. Finally, recently $\Delta^9$-tetrahydrocannabinol (THC) was used to demonstrate that hTRPV2 was a functional channel (Neeper et al., 2007). We confirm this observation; THC activates hTRPV2 with an apparent affinity close to that of mTRPV2 (Fig. 4C). These results clearly demonstrate that hTRPV2 lacks 2APB sensitivity but is a functional channel as initially shown (Neeper et al., 2007).

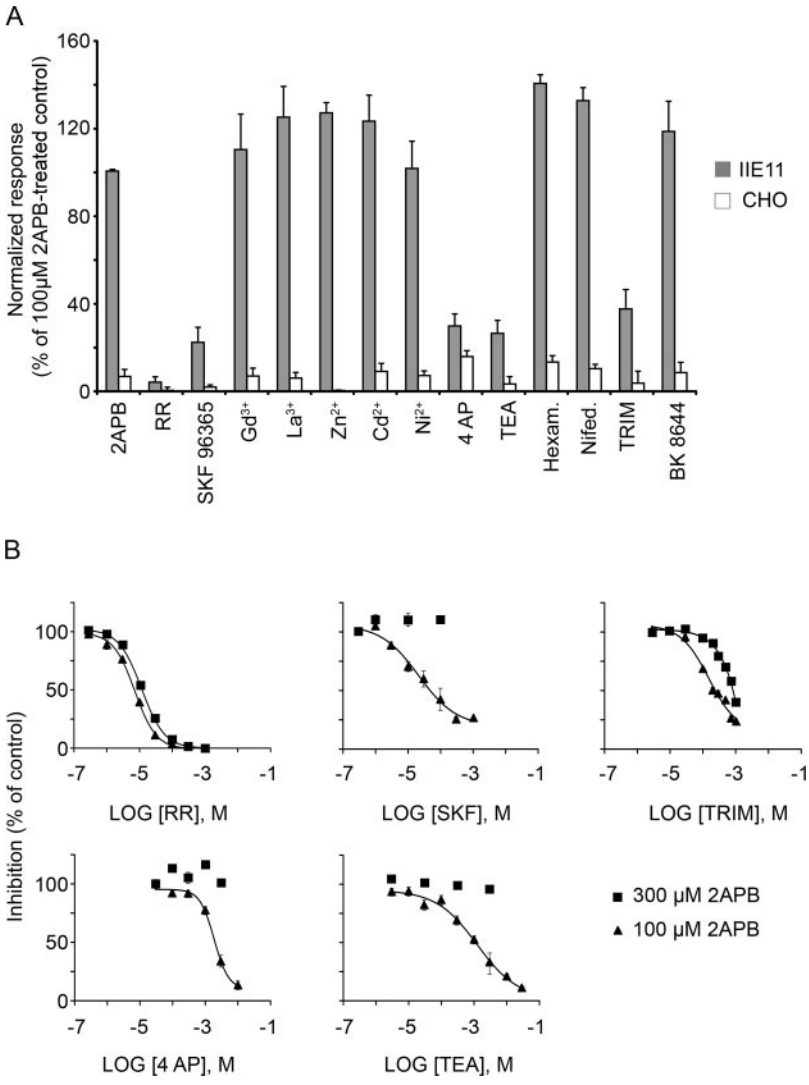


**Fig. 2.** Characterization of TRPV2 channel blockers. A, inhibition levels of 2APB-induced calcium signals by different chemicals. Chemicals were coapplied with 100 μM 2APB at a concentration of 100 μM except for TEA and 4-AP (1 mM) and TRIM (500 μM). Results were normalized to the fluorescent signal induced in clone IIE11 by 100 μM 2APB applied alone. Each measurement was made in triplicate and averaged; results are mean ± S.E.M. of at least three experiments. B, inhibitory dose-response experiments for the five identified inhibitors. Increasing concentrations of inhibitor were coapplied with either 100 μM (▲) or 300 μM 2APB (■). Fluorescence was normalized to the 2APB-induced signal in the absence of inhibitor.

**Molecular Determinants of 2APB Sensitivity.** We took advantage of the sequence similarity between mouse and human channels to identify the molecular determinants of 2APB sensitivity through chimera construction and analysis. Four modules were defined in TRPV2: the cytoplasmic amino terminus, transmembrane domains (TMD) from TM1 to TM5, the pore region from TM5 to the end of TM6, and the carboxyl terminus region (Fig. 5A). Modules from each channel were swapped individually or in combination. Proper expression and membrane localization of all chimeras were analyzed by immunostaining. We first investigated whether the reciprocal transfer of the pore region affected the 2APB sensitivity of the resulting chimera. As shown in Fig. 5B, mTRPV2 channels comprising the human pore region (chimera 1) are fully functional, whereas the mouse pore region does not confer 2APB sensitivity to the human channel (chimera A). This demonstrates that the 2APB binding site is not localized to the pore-forming region. This also rules out the possibility that the sequence differences in the TM5–TM6 linker of the human channel are responsible for a permeation deficiency.

In a second series of chimeras, amino and carboxyl termini were individually swapped. None of these chimeras was functional, but none of the chimeras associating the carboxyl terminus of hTRPV2 with the amino terminus of mTRPV2 were able to reach the plasma membrane (chimeras 3 and B). We therefore swapped both cytoplasmic regions. In this case, chimera D, which carries the human TMD and both mouse cytoplasmic regions, was found to be sensitive to 2APB. The mirror chimera 4 (mouse TMD with human cytoplasmic regions) was not sensitive to 2APB, despite being correctly localized to the plasma membrane.

The trafficking deficit of chimeras 3 and B prevented us from examining the individual contribution of cytoplasmic regions to 2APB sensitivity. However, we noticed that the last 35 amino acids of the human and mouse TRPV2 are very divergent (see Supplementary Fig. S2). We therefore tested whether this stretch of amino acids could be involved either in 2APB sensitivity and/or in the trafficking of the channels. Swapping this minimal region between mouse and human channels had no effect on 2APB sensitivity (Fig. 5B; chimeras 5 and F) but did restore membrane expression of the two trafficking-deficient chimeras 3 and B (Fig. 5C; chimeras 6 and G). These data suggested that 2APB sensitivity may involve both amino and carboxyl termini of the mouse channel. If so, coexpressing chimeras that individually contribute either the N or the C terminus of mTRPV2 should lead to partial 2APB sensitivity. Indeed, this is what was observed upon coexpression of pairs of inactive chimeras (2 + B), (3 + C), and (B + C); each of these combinations led to functional, 2APB-sensitive channels, albeit with lower efficacy (Fig. 5D).

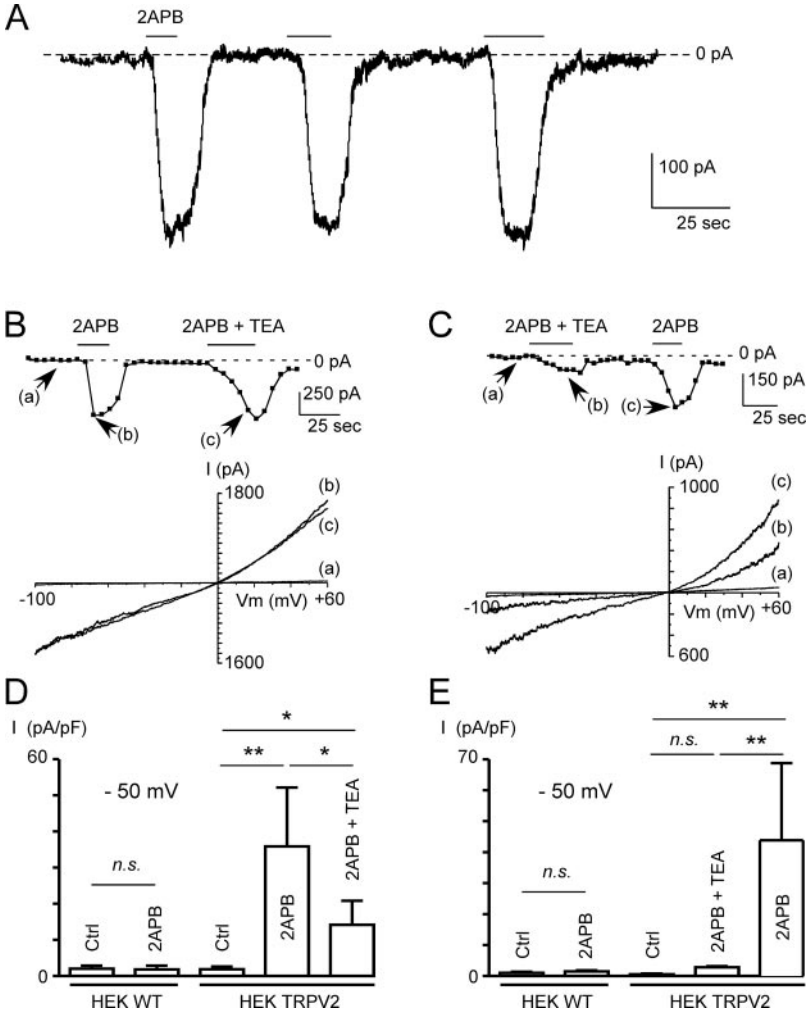


**Fig. 3.** 2APB-evoked mTRPV2 currents and inhibition by TEA. A, mTRPV2 was transiently transfected in HEK cells and experiments were performed 48 h later. Whole-cell currents evoked by 3 mM 2APB were recorded at a holding potential of −80 mV. 3 mM 2APB was applied for 10 s through a rapid perfusion system, every 20 to 30 s. Currents showed no desensitization either during 2APB application or after repetitive stimulations. B to E, use-dependence of TEA inhibition. Currents were recorded during 900-ms voltage ramps from −100 to +60 mV applied every 5 s. Cells were stimulated either first by 2APB and then by 2APB plus TEA (B and D) or first by 2APB plus TEA and then by 2APB (C and E). B, and C, top, chart recording of current intensities measured at −50 mV; horizontal bars indicate drug applications. Bottom, recordings of currents elicited by voltage ramps before (a) or during drug application (b and c) at times indicated in the top panel. D and E, current densities induced by 2APB or 2APB plus TEA measured at −50 mV in mTRPV2 transfected and control cells. Note that when TEA is coapplied with 2APB before any other stimulation (E), current densities are not different from baseline. 2APB had no effect on non transfected cells. One-way analysis of variance combined with a Newman-Keuls post test were used to compare the different values. n.s., not significant; *, $p < 0.05$; **, $p < 0.01$. Results are presented as mean ± S.E.M.

In addition, these coexpressions also corrected the trafficking deficit of chimeras 3 and B (Fig. 5E).

**Use of hTRPV2 to Probe Rodent TRPV2 Functions.** The insensitivity of hTRPV2 to 2APB could provide a tool to investigate cellular functions of TRPV2 channels of other species. To test this possibility, we constructed lentiviral vectors expressing either hTRPV2 or an hTRPV2[mut] cDNA that carried three mutations (E599K, M607K, and E609K) in the pore-selectivity filter. This mutated hTRPV2 was shown previously to behave as a dominant-negative mutant on mTRPV2 activity (Penna et al., 2006). We tested the ability of both lentiviruses to inhibit 2APB activation of mTRPV2. 2APB dose-response experiments were performed on clone IIE11 and CHO cells, transduced or not with hTRPV2 or hTRPV2[mut]-expressing lentiviruses. As shown in Fig. 6, overexpression of hTRPV2 induced a significant reduction of 2APB potency (▲): 2APB $EC_{50}$ values were 110 ± 20 and 180 ± 25 $\mu$M ($n = 3$) for control and hTRPV2-transduced cells, respectively ($p < 0.05$, paired Student's $t$ test). Maximal responses to 2APB were also affected, suggesting that 2APB might act cooperatively to activate mTRPV2 and that full activation can only be reached when all subunits of the channel are sensitive to 2APB. Although not significant compared with hTRPV2-transduced cells, apparently stronger inhibitory effects were observed in cells expressing hTRPV2[mut] (Fig. 6, ▼); the $EC_{50}$ for 2APB in hTRPV2[mut]-transduced cells was 209 ± 17 $\mu$M ($n = 3$). A similar shift in potency was observed for DPBA in cells transduced with wild-type and mutant hTRPV2-expressing viruses (Fig. 6, right).

**Activation of Native TRPV2 by 2APB.** TRPV2 has been reported to be expressed in the rat mast cell line RBL-2H3 (Stokes et al., 2004), and 2APB also has been shown to induce cationic currents in these cells (Braun et al., 2003). To investigate whether 2APB could activate native TRPV2 channels in these cells, we compared 2APB-induced calcium signals in naive RBL-2H3 cells and in cells transduced with lentiviruses expressing either GFP, wild-type hTRPV2, or hTRPV2[mut]. As shown in Fig. 7A, native TRPV2 proteins in RBL-2H3 are clearly localized at the plasma membrane and in punctated intracellular compartments; a similar pattern was observed in cells transduced with hTRPV2. Expression of endogenous TRPV2 proteins was also confirmed by Western blotting. TRPV2 was identified as a double band (presumably a glycosylated and unglycosylated forms) with a molecular mass of 85 kDa. Expressions of transduced hTRPV2 (either wild type or mutant) or control virus were confirmed by immunostaining and Western blotting using specific antibodies (Fig. 7A). These different cell populations expressing endogenous TRPV2 channels or transduced proteins were exposed to 2APB, and calcium signals were measured. In naive or GFP-transduced cells, 2APB induced a dose-dependent calcium signal with an $EC_{50}$ value of 257 ± 16 $\mu$M ($n = 4$) and 269 ± 30 $\mu$M ($n = 4$), respectively. For DPBA, $EC_{50}$ values were 209 ± 34 $\mu$M ($n = 4$) and 188 ± 35 $\mu$M ($n = 4$) in naive and GFP-transduced cells, respectively. As expected, transduction with hTRPV2 and hTRPV2[mut] caused a reduction of both $EC_{50}$ values and the maximal response to 2APB (Fig. 7B, left). In hTRPV2-transduced cells, $EC_{50}$ values for 2APB and DPBA were 812 ± 146 $\mu$M ($n = 4$) and 520 ± 120 $\mu$M ($n = 4$), respectively. These values were significantly different from those obtained in naive cells ($p < 0.005$ and $< 0.05$, unpaired Student's $t$ test, for 2APB and DPBA, respectively). Transduction with hTRPV2[mut] induced a significantly higher inhibition of 2APB-evoked maximal responses than transduction with hTRPV2 ($p < 0.05$, Student's $t$ test), further demonstrating its dominant-negative behavior.

RBL-2H3 cells express high-affinity receptors (FceRI) for

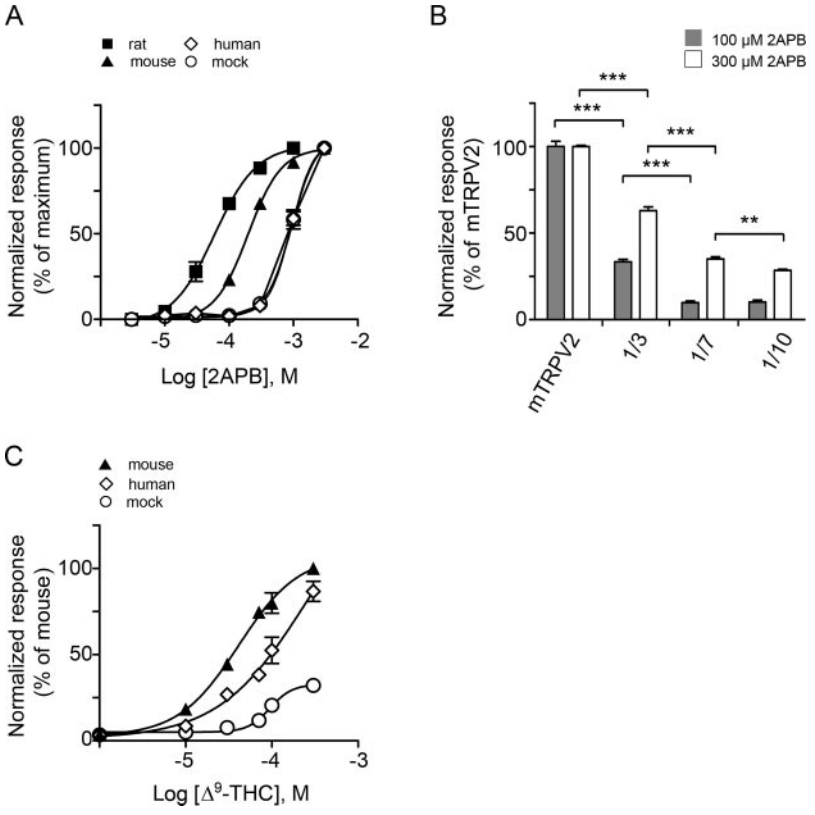


**Fig. 4.** Lack of activation of hTRPV2 by 2APB. A, 2APB dose-response curves for rat, mouse, and human TRPV2 transiently expressed in CHO cells. Fluorescent signals were normalized to the maximal response obtained for each channel. Note that there is no difference between nontransfected and hTRPV2 transfected cells. B, hTRPV2 inhibits 2APB activation of mTRPV2 when both channels are coexpressed. mTRPV2 and hTRPV2 were transiently coexpressed at different cDNA ratios; the amount of mTRPV2 cDNA was kept constant, whereas that of hTRPV2 was increased. Cells were stimulated with 100 $\mu$M (▨) or 300 $\mu$M 2APB (□). After subtraction of nonspecific signals measured in nontransfected cells, results were normalized to 2APB-induced responses in cells transfected with mTRPV2 alone. C, mouse and human TRPV2 are activated by THC. Dose-response curves for THC in CHO cells transiently transfected with either mouse or human TRPV2 cDNA. **, $p < 0.01$, ***, $p < 0.001$, unpaired Student's $t$ test.

IgE, which, when aggregated, cause the release of inflammatory mediator-containing granules. It has been proposed that in RBL-2H3 cells, TRPV2-mediated calcium influx could participate to granule secretion and lead to serotonin release (Stokes et al., 2004). We tested this hypothesis in RBL-2H3 cells transduced with either hTRPV2- or mutant hTRPV2-coding viruses. After an overnight sensitization with an anti-DNP IgE antibody, FceRI aggregation was triggered by increasing DNP-HSA concentrations, and intracellular calcium signals and exocytosis caused by antigen binding were monitored using Fluo-4 AM and β-hexosaminidase assay, respectively. DNP-HSA-induced calcium signals were clearly not different between naive, GFP-, hTRPV2-, or hTRPV2[mut]-transduced cells (Fig. 7B, right), suggesting that calcium influx through TRPV2 is not involved in mast cell degranulation. The ability of 2APB to trigger degranulation from RBL-2H3 cells was tested by monitoring the activity of β-hexosaminidase, an enzyme stored in secretory granules of RBL-2H3 cells. In control RBL-2H3 cells, at concentrations lower than 1 mM, 2APB induced a dose-dependent increase of secretion that seemed to saturate (Fig. 7C, left). This secretion only reached 7% of total β-hexosaminidase cellular content compared with the 35% that was observed using a saturating concentration of DNP-HSA (Fig. 7C, right). Nevertheless, 2APB-induced secretion was significantly impaired in cells transduced with hTRPV2[mut], suggesting that activation of TRPV2 channels by 2APB could stimulate mast cell degranulation, albeit at very low levels. When DNP-HSA-triggered secretion was analyzed, overexpression of hTRPV2[mut] did not affect β-hexosaminidase release (Fig. 7c, right). Taken together, these results suggest that, in physiological conditions, calcium influx through TRPV2 channels does not participate to mast cell degranulation, although its direct activation by 2APB can evoke low levels of exocytosis.

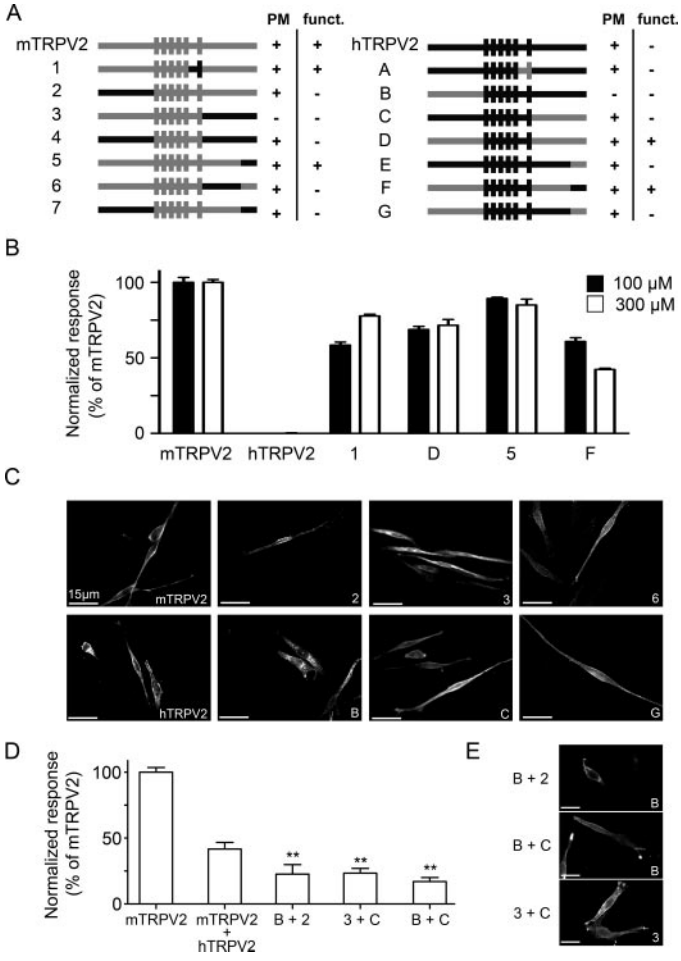


**Fig. 5.** Molecular determinants of 2APB sensitivity. A, diagram of the different chimeras tested; gray and black shading corresponds to mTRPV2 and hTRPV2 amino acid sequences, respectively; rectangles represent transmembrane domains. PM, plasma membrane expression; funct., function. B, 2APB-induced calcium responses of the different active constructions tested. cDNAs were transiently transfected in CHO cells, and experiments were performed 48 h later. Results were normalized to responses induced by 100 or 300 μM 2APB in mTRPV2-transfected cells. C, for each chimera, membrane expression was monitored by immunostaining. Note the clear intracellular localization of chimeras 3 and B compared with the others. D, partial 2APB sensitivity is restored when mTRPV2 amino and carboxy termini are brought by two independent subunits. Chimera cDNAs were transfected at the same ratio, and responses to 100 μM 2APB were measured 48 h later. Results were normalized to the 2APB-induced response obtained in mTRPV2-transfected cells. Note that coexpression of chimeras B and C lead to 2APB sensitivity, although these chimeras only carry either the N or the C terminus of mTRPV2. E, coexpression rescues the membrane expression of trafficking-deficient chimera. Analysis of the membrane expression of trafficking deficient chimeras 3 and B (white letters) was performed by immunostaining. Specific immunostaining was made possible through the use of species-specific antibodies directed against the divergent C-terminal sequence of either human or rat channels.

## Discussion

A subset of TRPV channels (TRPV1–V4) is known to be involved in sensory transduction (Caterina, 2007). Among them, TRPV2 still remains poorly characterized, mainly because of the lack of specific pharmacological and molecular tools. TRPV2 is highly expressed in human blood cells, suggesting that, in addition to its role as a noxious heat sensor (Caterina et al., 1999), this channel certainly encompasses other cellular functions (Saunders et al., 2007). Diphenyl borate derivatives have been identified as chemical activators of TRPV1 to -3 channels (Hu et al., 2004); in the case of TRPV3, these compounds have led to a better understanding of channel gating and have also proved to be useful tools to

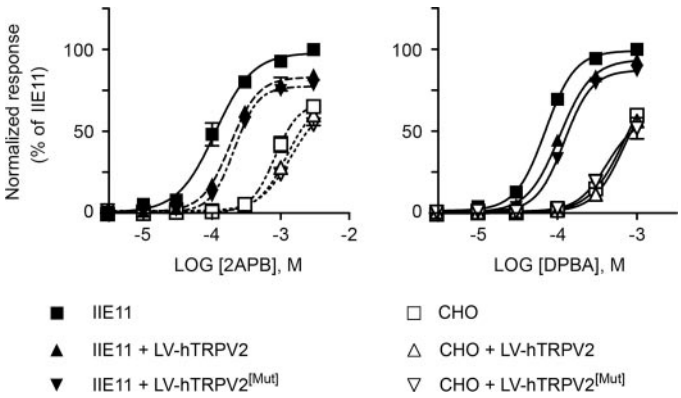


**Fig. 6.** Lentivirus expression of hTRPV2 inhibits mTRPV2 activation by 2APB in stably expressing cells. Lentivirus-driven expression of hTRPV2 inhibits 2APB and DPBA activation of stably expressed mTRPV2. IIE11 and parental CHO cells were transduced with a lentivirus expressing either hTRPV2 or hTRPV2[mut]; 5 days after transduction, dose-response curves for 2APB (left) or DPBA (right) were performed. hTRPV2 or hTRPV2[mut] expression induced a rightward shift in the dose-response curve for both agonists and a reduction of the maximal responses. For comparison purposes, results were normalized to the maximal response induced by 2APB or DPBA in nontransduced cells.

activate native channels in primary keratinocytes (Chung et al., 2004, 2005). In this study, we developed a calcium-based screening assay to further characterize TRPV2 pharmacology using 2APB and DPBA to activate the channel. Our results show that both compounds activate TRPV2 with a threshold in the range of 10 $\mu$M. In nontransfected cells (HEK or CHO), we observed a strong nonspecific calcium signal for agonist concentrations greater than 1 mM that was not additive with TRPV2-mediated calcium entry. We have no explanation for this lack of additivity, although one possibility is that high concentrations of 2APB induce membrane perturbations leading to calcium influx. Because of these limitations it is difficult to calculate precise values of the affinities of 2APB and DPBA for TRPV2 channels. However our $EC_{50}$ value estimations are consistent with previously reported values, indicating that 2APB activates TRPV2 and TRPV1 (Hu et al., 2004) within the same range of concentration. Activation of TRPV2 by other chemicals, including known activators of TRPV channels such as capsaicin, different bioactive lipids (arachidonic acid and its derivatives), or phorbol esters, was also tested. However, none of these molecules was active. In a recent report, THC was proposed to activate both human and rat TRPV2 with affinities in the micromolar range (Neeper et al., 2007). We here confirm this observation, although we did not investigate it further.

The screening for potential blockers of TRPV2 confirmed the inhibitory effect of known TRP channel blockers such as ruthenium red and SKF96365. We also found that two potassium channel blockers, TEA and 4-AP, inhibited TRPV2 with apparent affinities in the millimolar range. This result is surprising because these compounds are considered specific blockers of potassium channels. TEA and 4-AP binding sites have been localized in the $K_v$ family potassium channel pore-forming region, which shares significant sequence homology with that of TRPV proteins (Voets and Nilius, 2003). It is conceivable that TEA and 4-AP can block TRPV2 and potassium channels through similar mechanisms. One novel finding is the inhibitory effect of TRIM on 2APB-mediated activation of TRPV2. TRIM is described as an inhibitor of NO synthase (Handy et al., 1995) but also has an effect on store-operated calcium entry (Gibson et al., 2001). It is noteworthy

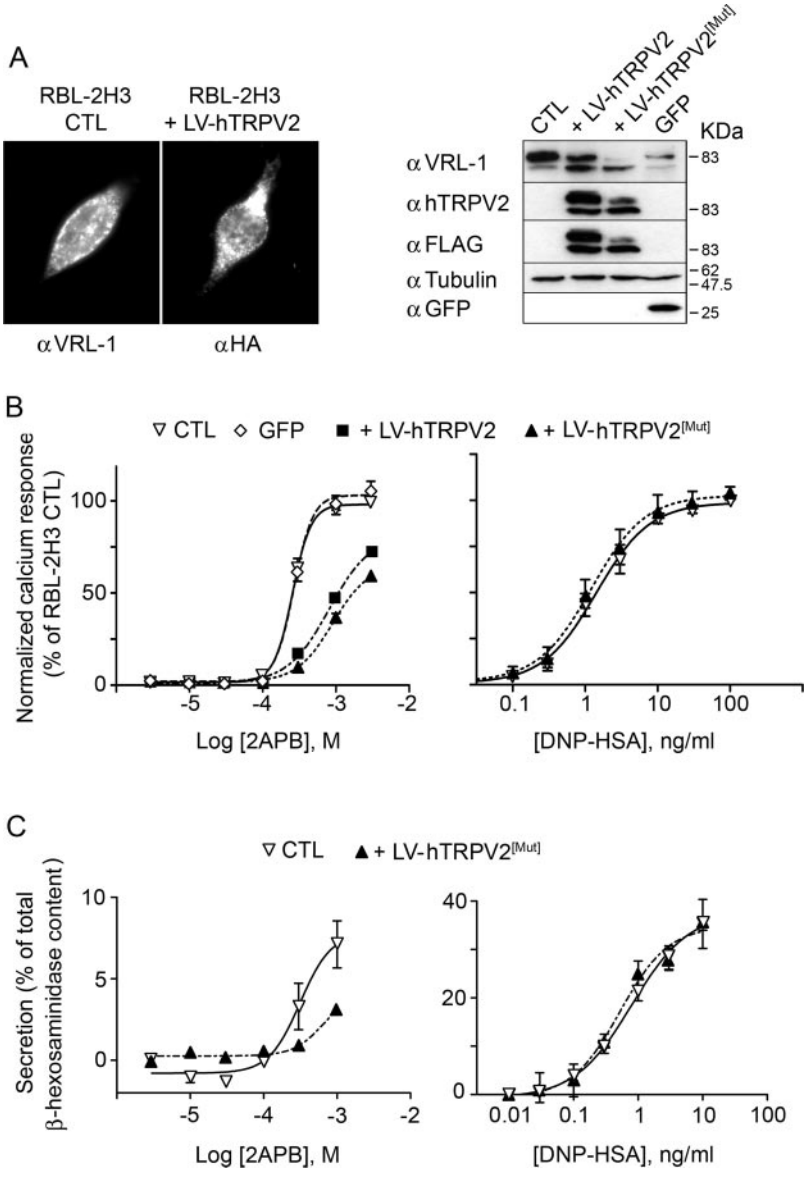


**Fig. 7.** Lentiviral-mediated hTRPV2 expression inhibits 2APB activation of endogenous TRPV2 in RBL-2H3 cells but not DNP-HSA-induced secretion. All hTRPV2 cDNAs were modified to carry an N-terminal flag and an extracellular HA epitope. A, left, immunostaining of endogenous rTRPV2 and of transduced Flag-hTRPV2$^{HA}$ in RBL-2H3 cells. Endogenous rTRPV2 was detected using the commercial VRL-1 antibody, whereas hTRPV2 was detected using anti-HA tag antibody. Right, Western blotting of endogenous rTRPV2, lentiviral-transduced GFP, wild-type hTRPV2, and hTRPV2[mut] in RBL-2H3 cells. Note the clear molecular mass difference between rat and human TRPV2 channels and the lack of cross-reactivity between VRL-1 and hTRPV2 antibodies. Tubulin was used as loading control. B, analysis of intracellular calcium increase induced by 2APB and DNP-HSA in transduced and nontransduced RBL-2H3 cells. 2APB-induced intracellular calcium increase is inhibited by overexpression of hTRPV2 or hTRPV2 carrying three mutations in the pore-selectivity filter. Note that GFP transduction does not affect 2APB-mediated calcium increase. After sensitization, DNP-HSA triggered an intracellular calcium increase that was not inhibited by hTRPV2 or hTRPV2[mut], indicating that TRPV2 is not involved in DNP-HSA-mediated calcium increase. C, 2APB-mediated TRPV2 activation induced low levels of $\beta$-hexosaminidase secretion. Left, low concentrations of 2APB induced a small dose-dependent increase of $\beta$-hexosaminidase secretion that is inhibited by overexpression of hTRPV2[mut]. Right, DNP-HSA-induced secretion is not inhibited by hTRPV2[mut] expression. Note that the secretion induced by DNP-HSA reaches 35% compared with 7% with 2APB. Results were normalized to intracellular $\beta$-hexosaminidase contents after substraction of basal secretion.

that TRIM inhibits oxytocin-induced neuronal firing in the supraoptic nucleus of the hypothalamus (Tobin et al., 2006), in which TRPV2 is highly expressed and localized on oxytocin neurons (Wainwright et al., 2004).

Another unexpected finding was the reduced effect of most of these blockers when TRPV2 was activated by 300 $\mu$M 2APB. One possible explanation is that these blockers act as competitive antagonists. However, our results suggest that the 2APB binding site is located intracellularly, implying that all competitive inhibitors would need to cross the plasma membrane to target the same site as 2APB. Although we cannot completely rule out this possibility, it is clearly not supported in the case of TEA, which is weakly membrane-permeant. Another interpretation could be that these inhibitory effects strongly depend on the cellular membrane potential and that activation by 300 $\mu$M 2APB induces a membrane depolarization strong enough to reduce channel inhibition. This is unlikely, because a depolarization induced by increasing the extracellular potassium concentration from 5 to 30 mM did not affect inhibition of either 100 or 300 $\mu$M 2APB-evoked calcium signals by SKF96365, TEA, or 4-AP (data not shown). In addition, patch-clamp recordings clearly show that the inhibitory effect of TEA does not depend on membrane potential but rather displays a strong use-dependence; indeed, TEA inhibition of 2APB-evoked currents consistently decreased upon repetitive stimulations. This raises the possibility that high concentrations of 2APB may induce progressive conformational changes of the channel that reduce the accessibility of the blockers to their binding site. On the other hand, these conformational changes could affect the pore selectivity of TRPV2 channels. Such selectivity changes induced by 2APB have been demonstrated in the case of TRPV3 gating (Chung et al., 2005). Further biophysical studies are necessary to understand the mechanism underlying this use-dependence.

One main result of this study is the lack of sensitivity of hTRPV2 to 2APB. This confirms previously published work showing that hTRPV2 did not respond to 2APB, whereas TRPV2 from rat is 2APB-responsive (Neeper et al., 2007). How could this lack of sensitivity be explained? The most likely hypothesis is that hTRPV2 is not activated by 2APB because of intrinsic properties of the protein. This is supported by the chimera experiments that clearly demonstrate that 2APB sensitivity can be transferred from the mouse to the human channel and is determined by intracytoplasmic regions. hTRPV2 shows the most divergence in a comparison of the sequences of the three TRPV2 homologs (21.2 and 24.8% against mouse and rat, respectively, whereas rat shows 7.5% divergence against mice). These amino acid differences are mostly clustered in the distal parts of both amino and carboxyl cytoplasmic regions (see Supplementary Fig. S2) and are likely to underlie 2APB sensitivity. Although extracellular TM1–TM2, TM3–TM4, and TM5–TM6 linkers also display sequence divergences, several chimeras containing the mouse TMD do not show any 2APB sensitivity, ruling out a possible contribution of TMD to 2APB sensitivity. Similar findings were discovered through chimeric studies using human-rat hybrid channels (Neeper et al., 2007). Our results further extend these observations to mouse-human chimeras.

Our results provide some insight on the mechanism of action of 2APB. First, they demonstrate that the 2APB binding site is unlikely to be extracellular, as proposed previously (Hu et al., 2004), but rather located intracellularly, because 2APB gating is only observed when both intracytoplasmic regions of mTRPV2 are present. This is compatible with the hydrophobic nature of 2APB, which is known to be able to reach intracellular targets such as inositol 1,4,5-triphosphate receptors (Missiaen et al., 2001). Our data also show that hTRPV2 exerts a dominant-negative inhibitory effect on 2APB gating. Indeed, lentiviral expression of hTRPV2 and the mixing experiments induce both a reduction of both maximal response and apparent affinity of 2APB for mTRPV2. This raises the possibility that conformational changes of mTRPV2 subunits induced by 2APB lead to the opening of the channel, and these changes are impaired when an hTRPV2 subunit is present in the protein complex. These conformational changes might be a direct consequence of 2APB binding to the channel. On the other hand, 2APB might act indirectly via intracellular proteins that specifically interact with rodent TRPV2 channels or through specific post-translational modifications of the channels. Assuming that 2APB gates TRPV1, -V2, and -V3 through similar mechanisms, it is easier to interpret our results by a direct binding of 2APB to the channels rather than through a common interacting protein or post-translational modifications.

2APB is an interesting tool to apprehend the physiological function of native TRPV2 channels. TRPV2 is expressed in the RBL-2H3 mast cell line, where it has been proposed to be involved in the exocytosis of granule contents. 2APB also induces cationic channel activity in these cells (Braun et al., 2003). Our results clearly show that in RBL-2H3 cells, 2APB induces an intracellular calcium increase that can be reduced by overexpression of hTRPV2. However, 2APB induces minimal degranulation of sensitized RBL-2H3 cells compared with a physiologically triggered secretion. Furthermore, DNP-HSA-induced secretion was not affected by transduction of cells with lentiviruses encoding hTRPV2 or inhibited by overexpression of a pore mutant channel with known dominant-negative effects (García-Martínez et al., 2000; Penna et al., 2006). This strongly argues against the involvement of TRPV2-mediated calcium entry in degranulation or secretion mechanisms in mast cells. Further investigations are undoubtedly required to understand the cellular functions of TRPV2.

Thus, TRPV2 remains a channel with enigmatic functions, highly expressed in immune cells and in neurons. In this study, we provided new insights on the pharmacology of TRPV2 as well as molecular tools that should help decipher these functions. In addition, this work confirms that hTRPV2 has a specific pharmocological signature (Neeper et al., 2007). As such, these findings greatly oppose the widely held belief that TRPV2 responses are universal across mammalian species.

**Acknowledgments**

This work was made possible thanks to the pharmacology-screening facility of Institut Fédératif de Recherche 3 and to the Montpellier RIO Imaging facility. RBL-2H3 cells were provided by Dr. U. Blank (Institut Pasteur, Paris, France). We thank Drs. T. Durroux and I. A. Lefevre for their comments on the manuscript and P. Atger for help with figures.

## References


Benham CD, Davis JB, and Randall AD (2002) Vanilloid and TRP channels: a family of lipid-gated cation channels. *Neuropharmacology* **42:**873–888.

Braun FJ, Aziz O, and Putney JW Jr (2003) 2-aminoethoxydiphenyl borane activates a novel calcium-permeable cation channel. *Mol Pharmacol* **63**:1304–1311.

Caterina MJ (2007) Transient receptor potential ion channels as participants in thermosensation and thermoregulation. *Am J Physiol Regul Integr Comp Physiol* 292:R64–R76.

Caterina MJ, Rosen TA, Tominaga M, Brake AJ, and Julius D (1999) A capsaicin-receptor homologue with a high threshold for noxious heat. *Nature* **398:**436–441.

Chung MK, Guler AD, and Caterina MJ (2005) Biphasic currents evoked by chemical or thermal activation of the heat-gated ion channel, TRPV3. *J Biol Chem* **280:** 15928–15941.

Chung MK, Lee H, Mizuno A, Suzuki M, and Caterina MJ (2004) 2-aminoethoxydiphenyl borate activates and sensitizes the heat-gated ion channel TRPV3. *J Neurosci* **24:**5177–5182.

Clapham DE (2003) TRP channels as cellular sensors. *Nature* **426:**517–524.

García-Martínez C, Morenilla-Palao C, Planells-Cases R, Merino JM, and Ferrer-Montiel A (2000) Identification of an aspartic residue in the P-loop of the vanilloid receptor that modulates pore properties. *J Biol Chem* **275:**32552–32558.

Gibson A, Fernandes F, Wallace P, and McFadzean I (2001) Selective inhibition of thapsigargin-induced contraction and capacitative calcium entry in mouse anococcygeus by trifluoromethylphenylimidazole (TRIM). *Br J Pharmacol* **134:**233–236.

Handy RL, Wallace P, Gaffen ZA, Whitehead KJ, and Moore PK (1995) The antinociceptive effect of 1-(2-trifluoromethylphenyl) imidazole (TRIM), a potent inhibitor of neuronal nitric oxide synthase in vitro, in the mouse. *Br J Pharmacol* **116:**2349–2350.

Hardie RC (2001) Phototransduction in *Drosophila melanogaster*. *J Exp Biol* **204:** 3403–3409.

Hu HZ, Gu Q, Wang C, Colton CK, Tang J, Kinoshita-Kawada M, Lee LY, Wood JD, and Zhu MX (2004) 2-Aminoethoxydiphenyl borate is a common activator of TRPV1, TRPV2, and TRPV3. *J Biol Chem* **279:**35741–35748.

Iwata Y, Katanosaka Y, Arai Y, Komamura K, Miyatake K, and Shigekawa M (2003) A novel mechanism of myocyte degeneration involving the $Ca^{2+}$-permeable growth factor-regulated channel. *J Cell Biol* **161:**957–967.

Kanzaki M, Zhang YQ, Mashima H, Li L, Shibata H, and Kojima I (1999) Translocation of a calcium-permeable cation channel induced by insulin-like growth factor-I. *Nat Cell Biol* **1:**165–170.

Klages N, Zufferey R, and Trono D (2000) A stable system for the high-titer production of multiply attenuated lentiviral vectors. *Mol Ther* **2:**170–176.

Missiaen L, Callewaert G, De Smedt H, and Parys JB (2001) 2-Aminoethoxydiphenyl borate affects the inositol 1,4,5-trisphosphate receptor, the intracellular $Ca^{2+}$ pump and the non-specific $Ca^{2+}$ leak from the non-mitochondrial $Ca^{2+}$ stores in permeabilized A7r5 cells. *Cell Calcium* **29:**111–116.

Montell C (2005a) TRP channels in *Drosophila* photoreceptor cells. *J Physiol* **567:** 45–51.

Montell C (2005b) The TRP superfamily of cation channels. *Sci STKE* **2005:**re3.

Muraki K, Iwata Y, Katanosaka Y, Ito T, Ohya S, Shigekawa M, and Imaizumi Y (2003) TRPV2 is a component of osmotically sensitive cation channels in murine aortic myocytes. *Circ Res* **93:**829–838.

Naldini L, Blomer U, Gage FH, Trono D, and Verma IM (1996) Efficient transfer, integration, and sustained long-term expression of the transgene in adult rat brains injected with a lentiviral vector. *Proc Natl Acad Sci U S A* **93:**11382–11388.

Neeper MP, Liu Y, Hutchinson TL, Wang Y, Flores CM, and Qin N (2007) Activation properties of heterologously expressed mammalian TRPV2: evidence for species dependence. *J Biol Chem* **282:**15894–15902.

Penna A, Juvin V, Chemin J, Compan V, Monet M, and Rassendren FA (2006) PI3-kinase promotes TRPV2 activity independently of channel translocation to the plasma membrane. *Cell Calcium* **39:**495–507.

Ramsey IS, Delling M, and Clapham DE (2006) An introduction to TRP channels. *Annu Rev Physiol* **68:**619–647.

Saunders CI, Kunde DA, Crawford A, and Geraghty DP (2007) Expression of transient receptor potential vanilloid 1 (TRPV1) and 2 (TRPV2) in human peripheral blood. *Mol Immunol* **44:**1429–1435.

Stokes AJ, Shimoda LM, Koblan-Huberson M, Adra CN, and Turner H (2004) A TRPV2-PKA signaling module for transduction of physical stimuli in mast cells. *J Exp Med* **200:**137–147.

Tobin V, Gouty LA, Moos FC, and Desarmenien MG (2006) A store-operated current (SOC) mediates oxytocin autocontrol in the developing rat hypothalamus. *Eur J Neurosci* **24:**400–404.

Tominaga M and Caterina MJ (2004) Thermosensation and pain. *J Neurobiol* **61:**3–12.

Voets T and Nilius B (2003) The pore of TRP channels: trivial or neglected? *Cell Calcium* **33:**299–302.

Wainwright A, Rutter AR, Seabrook GR, Reilly K, and Oliver KR (2004) Discrete expression of TRPV2 within the hypothalamo-neurohypophysial system: implications for regulatory activity within the hypothalamic-pituitary-adrenal axis. *J Comp Neurol* **474:**24–42.


**Address correspondence to:** Dr. François-A Rassendren, Department of Molecular Pharmacology, Institut de Génomique Fonctionnelle, 141 rue de la Cardonille, 34094 Montpellier, France. Email: far@igh.cnrs.fr